INTERACTION BETWEEN NESFATIN-1 AND OXYTOCIN IN THE MODULATION OF THE SWALLOWING REFLEX

Florent Guillebaud, Guenièvre Roussel, Bernadette Félix, Jean-Denis Troadec, Michel Dallaporta, Anne Abysique

INTERACTION BETWEEN NESFATIN-1 AND OXYTOCIN IN THE MODULATION OF THE SWALLOWING REFLEX

Guillebaud Florent[1], Roussel Guenièvre[1], Félix Bernadette[2], Troadec Jean-Denis[1], Dallaporta Michel[1], and Abysique Anne [1,#]

1 : Université Aix Marseille. Laboratoire de Neurosciences Cognitives (LNC), UMR CNRS 7291. France
florent.guillebaud@univ-amu.fr
guenievre.roussel@univ-amu.fr
j-d.troadec@univ-amu.fr
michel.dallaporta@amu.fr
2 : Université Aix Marseille. Laboratoire de Physiologie et Physiopathologie du Système Nerveux (PPSN), EA 4674. France
bernadette.felix@univ-amu.fr

Correspondance to:
Abysique Anne, Université Aix-Marseille, Laboratoire de Neurosciences Cognitives, UMR CNRS 7291, Faculté des Sciences et Techniques de St Jérôme, Avenue Escadrille Normandie-Niemen, 13397 Marseille cedex 20, France. anne.abysique@univ-amu.fr.

Running title: Inhibition of the swallowing reflex by nesfatin-1

Abstract

Nesfatin-1, an 82-amino acid peptide encoded by the secreted precursor nucleobinin-2 (NUCB2), exerts potent anorexigenic action independently of leptin signaling. This propensity has propelled this peptide and its analogues as potential anti-obesity drug candidates. However, a more extensive comprehension of its biological actions is needed prior to envisaging its potential use in the treatment of metabolic diseases. Swallowing is an essential motor component of ingestive behavior, which induces the propulsion of the alimentary bolus from the mouth to the esophagus. The dorsal swallowing group (DSG) which constitutes a part of the central pattern generator of swallowing (SwCPG) is located within the solitary tract nucleus (STN), a region reported to contain nesfatin-1/NUCB2 expressing neurons. In this context, we investigate here the possible effects of nesfatin-1 on swallowing discharge. Nesfatin-1 dose-dependently inhibited swallowing reflex and activated neurons located in the DSG region. In addition, we provide evidences that strongly suggest that this nesfatin-1 inhibitory effect involved an oxytocinergic relay. Indeed, oxytocin (OT) injection at the brainstem level inhibited swallowing reflex and OT receptor antagonist prevented nesfatin-1 inhibitory action. Altogether, these data constitute the first demonstration that nesfatin-1 modulates swallowing reflex by acting at the brainstem level via an oxytocinergic relay.

Keywords: Superior laryngeal nerve, electrophysiology, solitary tract nucleus, central pattern generator of swallowing, vasotocin.

1. Introduction

Nesfatin-1 is an 82-amino acid peptide encoded by the secreted precursor nucleobinin-2 (NUCB2), reported to inhibit food intake via modulation of neuropeptides in the feeding centers of rodent brain (Oh-I et al., 2006). Nesfatin-1 quickly aroused community interest as it was shown that its action was independent of leptin signaling (Goebel et al., 2011; Oh-I et al., 2006; Shimizu et al., 2009a). Indeed, given the well-known leptin resistance that occurs in obese individuals, this propensity has propelled this peptide and its analogues as potential anti-obesity drug candidates. In addition, in humans, the modulation of nesfatin-1 expression was reported in various metabolic conditions, so that it could be considered as a potential biomarker for obesity (Dogan et al., 2016; St-Pierre et al., 2016; Tsuchiya et al., 2010). For instance, a significant negative correlation between plasma concentrations of nesfatin-1 and BMI, body fat percentage, and body fat weight was described in healthy non-obese individuals (BMI < 25 kg/m^2) (Tsuchiya et al., 2010). Furthermore, these authors reported significantly lower fasting concentrations of plasma nesfatin-1 in a group of high BMI (BMI > 28 kg/m^2) subjects compared to non-obese subjects (Tsuchiya et al., 2010). This negative correlation between nesfatin-1 and BMI also suggests that overweight or obesity could result from a deficiency of nesfatin-1 and thus that increasing the plasma nesfatin-1 concentration in the body could result in reduced body fat mass. Like-minded, it was shown that morbidly obese patients who had undergone laparoscopic sleeve gastrectomy exhibited significant increases in nesfatin-1 hormone levels in parallel to weight loss (Dogan et al., 2016). Accordingly, the therapeutic use of nesfatin-1 was envisaged for the treatment of obesity and associated co-morbidities (Ayada et al., 2015; Shimizu et al., 2009b). However, a deeper and comprehensive understanding of specific effects of nesfatin-1 is critical prior to envisaging its potential use in the detection and treatment of metabolic diseases. Indeed, nesfatin-1 was reported to exert multiple and diverse biological actions. Thus, nesfatin-1 regulates insulin secretion, adipocyte differentiation, gastric motility and arterial pressure (see (Wang et al., 2016); (Ramesh et al., 2017) for review). In accordance, nesfatin-

1/NUCB2 expression was described in diverse peripheral tissue including pancreas (Mohan and Unniappan, 2012), adipocyte (Ramanjaneya et al., 2010), stomach (Chung et al., 2013), intestine (Zhang et al., 2010) and heart (Feijoo-Bandin et al., 2013).

Swallowing is an essential motor component of ingestive behavior, which induces the propulsion of the alimentary bolus from the mouth to the esophagus and involves various muscles localized in the mouth, larynx, pharynx and esophagus. The superior laryngeal nerve (SLN) contains the sensory afferent fibers involved in the swallowing reflex. The afferent fibers contact interneurons located rostrocaudally within the medial part of the lateral NTS defined as the intermediate-subpostremal portion of this nucleus. This region overlaps with the interstitial, intermediate, ventral, and, to some extent, the ventrolateral subdivision of the NTS (Barraco et al., 1992). This neuronal population referred as the dorsal swallowing group (DSG) constitutes, with a ventral swallowing group located within the ventrolateral medulla above the nucleus ambiguous, the central pattern generator of swallowing (SwCPG) (Jean, 2001). Interestingly, previous works have shown that the swallowing reflex could be modulated by anorexigenic and orexigenic compounds (Abysique et al., 2015; Bariohay et al., 2008; Felix et al., 2006; Kobashi et al., 2010; Kobashi et al., 2014; Kobashi et al., 2017; Mostafeezur et al., 2012) suggesting that this motor component and the regulation of energy balance could be simultaneously targeted by the same effectors. For instance, leptin (Felix et al., 2006), ghrelin (Kobashi et al., 2010), brain derived neurotrophic factor (BDNF) (Bariohay et al., 2008) or glucagon like peptide-1 (Kobashi et al., 2017) were reported to inhibit the swallowing reflex after their central administration while cannabinoids facilitate the swallowing reflex elicited by the superior laryngeal nerve stimulation in rats (Mostafeezur et al., 2012).

In this context, the purpose of the present study was to perform the first investigation regarding the possible effects of nesfatin-1 on swallowing discharge. Since the anorexigenic action of central nesfatin-1 requires the recruitment of oxytocin neurons (Maejima et al., 2009; Nakata et al.,

2016; Saito et al., 2017; Yosten and Samson, 2010), we also tested a possible interaction between oxytocin and nesfatin-1 signaling in the control of swallowing.

2. Results

2.1. Inhibition of swallowing by nesfatin-1 administered into the DSG

Effects of nesfatin-1 were studied after central microinjections on 32 rats from 44 trials. The present results showed that nesfatin-1 induced a significant dose-dependent decrease in the number of swallows recorded during SLN stimulation. At 100 nM (22 rats, 22 trials), nesfatin-1 decreased the number of swallows with a short latency of 42.27 ± 4.70 s and this effect lasted for 12.11 ± 0.63 min (Fig. 1 and 2A). This effect was maximal for 10 minutes after nesfatin-1 injection ($P < 0.0001$) (Fig. 2A). At 50 nM (10 rats, 10 trials), nesfatin-1 also induced after a short latency of 51 ± 11.88 s a significant decrease in the number of swallows and this effect persisted for 13.35 ± 0.68 min (Fig. 2A). Compared with 100 nM, the maximal inhibitory effect presented similar amplitude ($P < 0.0001$) but lasted less time, only 4 minutes after microinjection. The effect of nesfatin-1 at 10 nM was investigated on the same rats used to study the effect of nesfatin-1 at 50 nM. In contrast, at this low dose (10 nM), nesfatin-1 did not modify the pattern of swallowing during SLN stimulation (10 rats, 12 trials). Therefore this dose could be considered as ineffective in our experimental conditions (Fig. 2A). Statistical comparison of the inhibitory effects of nesfatin-1 doses showed that inhibition time course was significantly different only between 100 nM and 10 nM and the difference between these two doses was significant between 2 and 12 minutes after microinjection (Fig. 2A). Nesfatin-1 administered within the DSG inhibited swallowing, without any variation of either cardiac frequency or respiratory activity (Fig. 1 and 2B-C).

2.2. Effects of 4th ventricle nesfatin-1 injection on c-Fos expression in the brainstem

Central structures activated in response to i.c.v. (4th ventricle) nesfatin-1 injection were identified using the immune detection of the c-Fos protein. A low basal level of c-Fos positive nuclei was observed in the brainstem of control (NaCl) rats (Fig. 3A-C). We firstly evaluated the effect of 100 nM nesfatin-1 on c-Fos expression since this dose induced a robust inhibition of swallowing. At this concentration, the ventricular injection of nesfatin-1 resulted in a modest but non-significant induction of c-Fos expression (data not shown). This negative result could be explained by a different route of administration used here i.e. intraventricular *vs* intraparenchymal. We next tested an higher nesfatin-1 dose i.e. 300 nM. This concentration was chosen since it was lower than concentrations reported to induce reduction of food intake after their intracerebroventricular administration (Oh-I et al., 2006; Stengel et al., 2009). Interestingly, at this concentration, treated rats exhibited an elevated number of c-Fos positive nuclei throughout the dorsal vagal complex (DVC, Fig. 3D-F) with a particular strong c-Fos labelling observed in STN regions surrounding the solitary tract (Fig.3G-H). Counts of positive nuclei in the STN revealed significant increases in the number of c-Fos labeled nuclei in treated animals compared with control animals whatever the sub-region of the STN considered i.e. rostral (NaCl : 8.3 +/- 3.2 *vs* nesfatin-1 : 18.0 +/- 4.3; $p < 0.001$), subpostremal (NaCl : 5.1 +/- 2.3 *vs* nesfatin-1 : 26.1 +/- 7.3; $p < 0.001$) and caudal (NaCl : 2.5 +/- 1.2 *vs* nesfatin-1 : 5.8 +/- 2.4 ; $p < 0.001$) parts (Fig. 3I). No labelling was observed outside the DVC including other brainstem nuclei and hypothalamus (data not shown).

2.3. Oxytocinergic terminals place alongside brainstem nesfatin-1/NUCB2 expressing neurons

We next performed oxytocin (OT) and nesfatin-1/NUCB2 double labelling on brainstem sections to evaluate the possible neuronal co-expression of these two peptides and/or the juxtaposition of

neuronal elements expressing OT and nesfatin-1/NUCB2. In contrary to hypothalamic nuclei where OT and nesfatin-1/NUCB2 were reported to co-localize in neuronal sub-populations (Goebel-Stengel and Wang, 2013), no localization was observed within the STN (Fig. 4A). Nevertheless, throughout the STN, including its lateral region comprising the DSG, OT positive fibers and varicosities were found in close apposition to nesfatin-1/NUCB2 expressing neurons (Fig. 4B and C). This closeness led us to consider a possible interaction between these two peptides at the brainstem level and in the context of swallowing control.

2.4. Oxytocin signaling and nesfatin-1-induced inhibition of the swallowing reflex

We investigated the effects of oxytocin (10 nM) on 11 rats from 13 trials. Microinjection of oxytocin in the DSG induced a significant decrease in the number of swallows recorded during SLN stimulation with a latency of 41.5 ± 5.41 s. This inhibitory effect was maximal for 4 minutes after oxytocin microinjection ($p<0.0001$) and persisted for 7.3 ± 1.44 min (Fig. 5 and 6A). Oxytocin administered within the DSG inhibited swallowing, without any variation of either cardiac frequency or respiratory activity (Fig. 5 and 6B-C). To investigate the possible involvement of oxytocin in the mechanism of the nesfatinergic inhibitory effect on swallowing reflex, we have studied the effects of the highest dose of nesfatin-1 after pre-treatment by vasotocin (OVT), an oxytocin receptor antagonist. Before OVT microinjection, nesfatin-1 (100 nM) induced a significant decrease in the number of swallows with a latency of 33 ± 3 s and a duration of 13.7 ± 0.92 min (10 rats, 10 trials, Fig. 7A and C). OVT (1 μM) was administered in the DSG 5 minutes before microinjection of nesfatin-1 (100 nM). In these conditions, nesfatin-1 did not modify the swallowing pattern discharge (10 rats, 10 trials, Fig. 7B and C). Moreover, OVT microinjected alone did not affect swallowing.

3. Discussion

In the present study, we observed for the first time that nesfatin-1 injected into the DSG is able to inhibit the swallowing reflex. Central administration of nesfatin-1 reduced the number of swallows in a dose-dependent and specific manner, without affecting other physiological functions (heart rate and respiratory activity). Whatever the dose of nesfatin-1 injected, the inhibitory action appeared with a short latency (<1 min) but this effect was relatively labile (~12-13 min). This duration was shorter when compared to other energy homeostasis-linked effectors reported to decrease swallowing i.e. leptin, BDNF (Bariohay et al., 2008; Felix et al., 2006). Interestingly, the nesfatin-1 doses able to modify swallowing frequency (50-100 nM) are consistent with endogenous nesfatin-1 levels reported within the rat hypothalamus and LCR (Oh-I et al., 2006). The pioneer work of Oh-I and colleagues (2006) reported a concentration of ~240 and 200 ng/ml within the hypothalamus and LCR respectively. Based on these values, we can approximate a nesfatin-1 concentration of ~ 24 and 20 nM within the hypothalamus and LCR respectively. Moreover, we also showed that 4^{th} ventricle nesfatin-1 injection resulted in a strong and significant increase in c-Fos expression within the STN including the DSG. This nesfatin-1-induced c-Fos expression was specific as it was absent in other brainstem or forebrain nuclei. Importantly, hypothalamic nuclei did not exhibit increased of c-Fos expression in response to 4^{th} ventricle nesfatin-1 administration. When nesfatin-1 was injected into the 4^{th} ventricle, its effects must have been larger than when injected in the DSG and in particular, it may have acted on the entire STN, involved in various autonomic functions. c-Fos data showed neuronal activation in various parts of the STN involved in autonomic functions including respiratory and cardiac functions. However, electrophysiological data did not present any variations of respiratory and cardiac activities. The data suggested that these functions were not affected by nesfatin-1 dose reaching the dedicated neurons. The subpostremal NTS level appears particularly sensible to icv nesfatin-1 injection. It's difficult to know why since the nesfatin-1 receptor or binding

site(s) remain unknown. Nevertheless, we can speculate that this region contains a large part of interneurons regulating not only swallowing but also food intake. Indeed, peripheral administration of anorexigenic nesfatin-1 dose (0,25 nmol/g of body weight), was reported to specifically induced c-Fos expression at the subpostremal NTS level after its peripheral injection (Shimizu et al., 2009a). Swallowing is the first motor component of the ingestive behavior and is essential for normal food intake; our results suggest that inhibition of swallowing by nesfatin-1 may contribute, at least in part, to the well-known anorexigenic effects of this substance.

To investigate the mechanism by which nesfatin-1 inhibits swallowing reflex, we aimed to establish the existence of interactions between nesfatin-1 and oxytocin signaling in this context of swallowing control. In addition to classical effects of oxytocin, numerous works have involved oxytocin in the regulation of feeding and energy expenditure. Evidences showed clearly that oxytocin acts as an anorexigenic hormone (Arletti et al., 1990; Olson et al., 1991; Yosten and Samson, 2010). Accordingly, animals deficient in oxytocin gene or genes related to the differentiation of oxytocin neurons exhibit hyperphagia and obesity (Kublaoui et al., 2008; Takayanagi et al., 2008). Moreover, several lines of evidences suggest that oxytocin may relay nesfatin-1 anorexigenic effects (Maejima et al., 2009; Price et al., 2008; Yosten and Samson, 2010). Nesfatin-1 exerts direct depolarizing action on oxytocinergic neurons and its central injection recruited both magnocellular and parvocellular oxytocin neurons which in turn stimulates oxytocin release (Price et al., 2008; Yosten and Samson, 2010). Altogether, these observations led to the conclusion that nesfatin-1 decreases food intake by activating oxytocinergic neurons. Here, we reported that the STN area corresponding to the DSG contains both oxytocin fibers and nesfatin-1 neurons which are often found in close apposition. In accordance, (Blevins et al., 2003) have clearly shown a high density of oxytocin projections in the medial subdivision of the STN, an area which includes the DSG. In parallel, we observed that oxytocin injection into the DSG inhibited significantly the swallowing reflex. Oxytocin

inhibited the swallowing reflex with a similar latency to nesfatin-1 while the inhibition duration was shorter. In the brain, the main sources of oxytocin are the magnocellular and parvocellular neurons of the paraventricular nucleus (PVN) and the supraoptic nucleus (Armstrong, 2004; Rosen et al., 2008). Moreover, in the rat, oxytocin receptors are abundantly present in several brain regions such as the hypothalamus and the brainstem (Gimpl and Fahrenholz, 2001). As described by several authors, there is a significant anatomical link between PVN and STN since PVN oxytocinergic neurons, particularly neurons of the posterior parvocellular subdivision, convey descending inputs from the hypothalamus to the STN neurons involved in food intake control (Blevins et al., 2003; Uchoa et al., 2013). Moreover (Rinaman, 1998) demonstrated by a retrograde transport of cholera toxin that all oxytocinergic neurons projecting to the STN originate from the PVN. *In vivo* experiments also demonstrated that electrical stimulation of the ipsilateral PVN triggered a release of oxytocin in the STN (Landgraf et al., 1990). Therefore, in our study, in regard to the inhibition of rhythmic swallowing induced by brainstem oxytocin administration, we can hypothesized that PVN oxytocinergic neurons could project to the STN area corresponding to the DSG and modulate the activity of the interneurons involved in the coordination of motor sequences necessary for swallowing reflex.

In our study, the inhibitory effect induced by the high nesfatin-1 dose was blocked by administration into the DSG of OVT, an oxytocin receptors antagonist. This suggests that the brainstem effects of nesfatin-1 on the swallowing reflex requires a release of oxytocin by the OT neurons endings. Remarkably, it was previously shown that intra-PVN nesfatin-1 injection induces c-Fos expression within the STN and that nesfatin-1 induced anorexia is blocked by 4^{th} ventricle injection of oxytocin receptor antagonist (Maejima et al., 2009; Yosten and Samson, 2010). Hence, the blockade of the nesfatin-1 inhibitory effect by OVT pre-treatment strongly suggests that nesfatin-1 stimulates locally (i.e. within the DSG) OT release from PVN-originating OT fibers.

In summary, our study demonstrates that nesfatin-1 inhibits the swallowing reflex in anesthetized rats. The nesfatin-1 mechanism of action appears to involve the oxytocin signaling. Nesfatinergic neurons, previously characterized in the STN by our team (Bonnet et al., 2009; Bonnet et al., 2013) and reported to be sensitive to inflammatory and glycemic related signals, may stimulate the release of oxytocin by the PVN neurons endings, and oxytocin may modulate swallowing by acting on the DSG.

4. Materials and methods

4.1. Ethical Statement

The experimental procedures were carried out in accordance with the directives of the French Ministry of Agriculture and Fisheries and the European Community Council (86/609/EEC). The protocol was approved by the committee on the ethics of animal experiments of Marseille/N°14 (authorization number: 01288.02).

4.2. Surgical and electrophysiological procedures

This study was performed on 43 adult male Wistar rats weighing 350 g (Charles River, l'Arbresle, France). The animals were anesthetized with 0.6 ml of a mixture of ketamine (100 mg/ml; Kétamine 1000 Virbac) and xylazine (20 mg/ml; Rompun, Bayer Santé, France), injected intraperitoneally in a proportion of 90% and 10%, respectively. The level of anaesthesia was maintained by perfusing the same mixture diluted at 10 % through a catheter inserted in the femoral vein, at a rate of 0.01-0.05 ml/h.

As previously described by (Abysique et al., 2015), the SLN was placed on bipolar electrodes included in a plexiglas gutter and, after craniotomy, the surface of the medulla was exposed in order to allow drugs microinjections in the intermediate STN which contains the DSG.

4.3. Drugs microinjections

As previously described by (Abysique et al., 2015), we used glutamate microinjection (1 fmol) as control to induce swallowing and to verify that the microelectrode was well positioned within the DSG. Then, these stereotaxic coordinates were conserved, and all drugs tested were microinjected in the DSG extending between 0.2-0.7 mm rostral to the caudal edge of the area postrema (taken as the 0), 0.5-0.7 mm laterally and 0.4-0.8 mm in depth.

The following drugs were used: nesfatin-1 (Phoenix Pharmaceuticals, France), oxytocin (Tocris, France) and oxytocin receptor antagonist: vasotocin/Compound IV/OVT (Phoenix Pharmaceuticals, France). Nesfatine-1, oxytocin and OVT were dissolved in NaCl 0.9% solution. As described by (Abysique et al., 2015), 100 nl of all the drugs were injected in the DSG by pressure ejections through glass micropipettes.

4.4. Stimulations and recordings

Swallowing was triggered by stimulation of the SLN. In this study, repetitive long trains of pulses (5 s duration at 15-30 Hz frequency every 30 s) were used and produced several swallows at a rhythm depending on stimulation frequency. The parameters of stimulation varied according to the animal (1.0-5.5 V; 0.02-0.8 ms) to induce a basal swallowing frequency comprised between 0.6 and 1.2 Hz. As described by (Abysique et al., 2015): *i*) the electromyographical (EMG) activity of sublingual muscles was recorded to monitor swallowing, *ii*) the respiratory activity and the electrocardiogram (ECG) were recorded to evaluate the level of anaesthesia and to determine any variation induced by drugs injection. Rectal temperature was monitored and maintained around 37°C with a heating pad. The EMG, ECG and respiration activity were recorded on a computer using an analog-to-digital interface (PowerLab 8SP data acquisition software for Windows, ADInstruments, USA).

4.5. Signal Analysis

A stable control sequence of swallowing involving three 5s trains of stimulations was recorded before each drug injection and the mean values calculated were used as control values. Stimulations and recordings were maintained until recovery. A specially designed computer program Chart5.5 software calculated: ∫EMG (electromyogram envelope signal normalized), Sw Number (number of swallows triggered by SLN stimulation), ECG and respiratory frequency. All swallows calculated values were normalized as percent of control values. ECG and respiratory frequencies were expressed as percent of control values recorded before each drug injection.

4.6. Surgery and intracerebroventricular injection of nesfatin-1

For cannula implantation, animals (n=6) were anesthetized by an intraperitoneal (ip) injection of ketamine (100 mg/ml, Ketamine 1000 Virbac, France) and xylazine (20 mg/ml; Rompun, Bayer Santé, France), and then placed in a digital stereotaxic apparatus (Model 502600, WPI) coupled to the neurostar software (Neurostar GmbH). A 26-gauge stainless steel cannula was implanted into the lateral ventricle at the following coordinates: 12.8 mm posterior to bregma, 0.2 mm lateral to the midline and 7.5 mm ventral to the skull surface. The cannula was secured to the skull with dental cement and sealed with removable obturators. The animals were sutured, placed in individual cages and allowed to recover for 7 days. During this resting period, animals were injected with physiological saline every other day for habituation. One week post-surgery, rats were administered 10 µl (2.5 µl/min) of either physiological saline (NaCl) or nesfatin-1 (300 nM) solution.

4.7. Immunohistochemistry

Animals treated by intracerebroventricular (icv) 10 µl injection of nesfatin-1 (300 nM, n=3) or NaCl (0.9 %, n=3) were used for immunostaining. Ninety minutes after injections rats under deep anesthesia were firstly perfused intracardially with ice-cold 0.1M phosphate buffered saline (PBS, pH 7.4) and then with ice-cold freshly prepared solution of 4 % paraformaldehyde (PFA) in 0.1M PB. The brains were immediately removed, post-fixed 1h in 4 % PFA at room temperature, rinsed overnight in PBS and then cryoprotected for 24 to 48h in 30 % sucrose at 4°C. The brains were frozen in isopentane (-40°C), then coronal sections (40 µm thick) of the brainstem were made with a cryostat (Leica CM3050, France) and collected serially in 0.1M PBS.

For c-Fos immunohistochemistry, brainstem sections were incubated for 10 minutes in 0.1M PBS containing 1.5 % H_2O_2 for quenching of endogenous peroxidase activity. After one hour in saturation PBS buffer containing 3% normal goat serum and 0.3 % triton X-100, sections were incubated for 48h at 4°C with a rabbit anti-c-Fos antibody (1/5000 Ab-5; Calbiochem). A biotinylated goat anti-rabbit IgG (1/400, Vector Labs) was used as a secondary antibody (incubated for 1h30 at room temperature). Peroxidase activity was revealed using the avidin-biotin complex (1/200, Vector Labs) and diaminobenzidine as chromogen. Non-specific labelling was observed on adjacent sections that were treated identically but without the primary antibody. The reaction was closely monitored and terminated by washing the sections in distilled water when optimum intensity was obtained (3-5 min). For each animal, c-Fos immunostaining photomicrographs were acquired using a 10 fold lens with a DMX 1200 camera (Nikon) coupled to ACT-1 software. The microscope was set at a specific illumination level, as was the camera exposure time. c-Fos positive nuclei were then counted on these pictures by computer-assisted morphometry using the ImageJ software.

To investigate relationships between nesfatinergic neurons and oxytocin fibers located in the DVC, we performed a double immunochemistry. Brainstem sections were treated with PBS containing 5 % donkey serum to block non-specific binding sites and 0.3 % triton X-100. Sections were incubated

overnight at room temperature with a primary antibody raised against nesfatin-1 (1/10000, Phoenix Pharmaceuticals), washed in PBS and then incubated for 2h at room temperature with a secondary antibody conjugated with Alexa 594 (1/400, Invitrogen). To identify oxytocin fibers, sections were then treated with PBS containing 3 % bovine serum albumin (BSA) to block non-specific binding sites and 0.3 % triton X-100. Sections were incubated overnight at room temperature with a primary antibody raised against oxytocin (1/1000, Millipore), washed in PBS and then incubated for 2h at room temperature with a secondary antibody conjugated with Alexa 488 (1/400, Life Technologies). Fluorescent images were acquired on a confocal microscope (Zeiss LSN 700) using the 488 nm band of an Ar-laser and the 543 nm band of an He/Ne-laser for excitation of Alexa-488 and Alexa-594, respectively. In double labeling experiments, images were sequentially acquired. All images were further processed in Adobe Photoshop 6.0, only contrast and brightness were adjusted.

4.8. Statistical analyses

For electrophysiogical data, statistical analyses were performed using one- or two-way analysis of variance (ANOVA) followed by Fisher's protected least-significant difference post-hoc test (StatView for Windows 5.0.1; SAS Institute). For c-Fos immunostaining, comparisons between data from vehicle and nesfatin-1 treated rats were performed using unpaired 2-tailed Student's t-test. All data were expressed as mean ±SEM. For all data, differences were considered significant when $P < 0.05$.

Acknowledgments: The authors acknowledge the Aix-Marseille University Microscopy Center CP2M for access to their confocal microscopy equipment and Kevin Poirot for his significant contribution to confocal images acquisition. The authors thank Jérôme Espejo for taking care of the animals.

Funding: This work was supported by funding obtained from the Aix-Marseille University, the Centre national de la Recherche Scientifique (CNRS) and the Institut National de la Recherche Agronomique (INRA).

Authors contributions

GF, RG, FB, DM and AA performed experiments. AA, FB, DM and TJD designed the study and analyzed data. AA, DM and TJD wrote the paper.

Figure Legends

Figure 1: Effects of nesfatin-1 injection on sublingual muscle electromyographical activity (EMG) induced by SLN stimulation and on cardiorespiratory activity.

Nesfatin-1 (100 nM) injected within the DSG induced a rapid and powerful inhibition of the number of swallows. 90 s after nesfatin-1 microinjection, only one swallow was triggered by SLN stimulation. This effect was transient since the swallows recovered after 16 minutes. Patterns of heart (ECG) and respiration rates were illustrated before and after nesfatin-1 injection (basal heart rate: 254.27±11.32/min, basal respiration rate: 95.87±6.58/min).

Figure 2: Specific and dose-dependent inhibition of triggered swallowing by nesfatin-1.

A: Time course of nesfatin-1 effects on the number of swallows after its injection within the DSG (100 nM : 22 trials, 50 nM :10 trials and 10 nM : 12 trials). Recordings were performed over 2 minutes periods until recovery. Note that at 10 nM, nesfatin-1 did not modify swallowing triggered by SLN stimulation.

B-C: Quantification of heart (**B**) and respiration (**C**) rates during nesfatin-1 application.

Time 0 represent the mean control value recorded before nesfatin-1 microinjection (100 %). Data are represented as means ± SEM normalized to the control value. * $P < 0.05$, *** $P < 0.001$, **** $P <$

0.0001 significantly different from control values. # P < 0.05, ## P < 0.01, ### P < 0.001, #### P < 0.0001 significant differences between 100 nM and 10 nM treated rats.

Figure 3: Effects of central nesfatin-1 administration on brainstem c-Fos immunoreactivity.

A-F: Representative coronal sections illustrating c-Fos labeling observed at different levels of the NTS of rats treated with NaCl 0.9 % (**A-C**) or nesfatin-1 300 nM (**D-F**) and sacrificed 1h30 post-treatment. Scale bar: 100 µm.

G-H: High magnification of images **B** and **E** illustrating the strong labelling observed in subpostremal STN regions surrounding the solitary tract. Scale bar: 50 µm.

I: Quantification of immunoreactive c-Fos nuclei in the brainstem of rats treated either with NaCl (0.9 %, gray bars) or nesfatin-1 (300 nM, black bars). ** P < 0.01, *** P < 0.001 significantly different from NaCl-treated rats; AP, area postrema; cc, central canal; STN, solitary tract nucleus; ts, solitary tract; X, Dorsal motor nucleus of the vagus; 4V, 4th ventricle.

Figure 4: Illustration of the strong spatial association between OT positive processes and nesfatin-1/NUCB2 expressing neurons.

A: Immunohistochemical double-labelling of nesfatin-1/NUCB2 and oxytocin (OT) performed on coronal sections of STN. **Arrows**: OT+ fibers. Scale bar: 30 µm. **B:** Higher magnification of OT and nesfastin-1/NUCB2 labelling in the STN. The area where the image originates is indicated by a rectangle in the low-power photomicrograph in **A**. Scale bar: 5 µm. **C:** Serial confocal images illustrating the close apposition of OT fibers and nesfatin-1/NUCB2 neurons. Scale bar: 5 µm.

AP, area postrema; STN, solitary tract nucleus; ts, solitary tract.

Figure 5: Effects of oxytocin central administration on swallowing triggered by SLN stimulation and on cardiorespiratory activity.

Oxytocin (10 nM) inhibited sublingual muscle electromyographical activity. 2 minutes after oxytocin microinjection within the DSG, only three swallows were triggered by SLN stimulation. This effect was transient since the swallows recovered after 9 minutes. Patterns of heart (ECG) and respiration rates were illustrated before and after oxytocin injection (basal heart rate: 280.77±19.20/min, basal respiration rate: 70.99±5.74/min).

Figure 6: Specific inhibition by oxytocin on triggered swallowing.

A: Time course of the effects of oxytocin (10 nM, 13 trials) microinjected within the DSG on the number of swallows recorded over 2 minutes periods and until recovery.

B-C: Quantification of heart (**B**) and respiration (**C**) rates during oxytocin application.

Time 0 represent the mean control value recorded before oxytocin microinjection (100%; black bars). Data are represented as means ± SEM normalized to the control value. ** $P < 0.01$, **** $P < 0.0001$.

Figure 7: Effects of nesfatin-1 central administration on swallows before and after OVT microinjection.

A: Before OVT microinjection, nesfatin-1 (100 nM, 10 trials) always induced a rapid and powerful inhibition of the number of swallows. 49s after nesfatin-1 microinjection, only two swallows were triggered by SLN stimulation. This effect was transient since the swallows recovered after 16 minutes.

B: After pre-treatment by OVT (1 μM), nesfatin-1 microinjection within the DSG no longer changed the number of swallows.

C: Time course of the effects of nesfatin-1 centrally administered (100 nM, 10 trials) on the swallowing reflex before and after pre-treatment by OVT (1 μM). The number of swallows was recorded over 2 minutes periods and until recovery. Time 0 represent the mean control value recorded before nesfatin-1 microinjection (100 %). Data are represented as means ± SEM normalized to the control value. ** P < 0.01, *** P < 0.001, **** P < 0.0001.

References

Abysique, A., Tardivel, C., Troadec, J.D., Felix, B., 2015. The Food Contaminant Mycotoxin Deoxynivalenol Inhibits the Swallowing Reflex in Anaesthetized Rats. PLoS One. 10**,** e0133355 DOI: 10.1371/journal.pone.0133355.

Arletti, R., Benelli, A., Bertolini, A., 1990. Oxytocin inhibits food and fluid intake in rats. Physiol Behav. 48**,** 825-30.

Armstrong, W.E., 2004. Hypothalamic supraoptic and paraventricular nuclei. In The rat Nervous system. Vol., G.P.S. Diego, ed.^eds. Elsevier Academic, pp. 369-388.

Ayada, C., Toru, U., Korkut, Y., 2015. Nesfatin-1 and its effects on different systems. Hippokratia. 19**,** 4-10.

Bariohay, B., Tardivel, C., Pio, J., Jean, A., Felix, B., 2008. BDNF-TrkB signaling interacts with the GABAergic system to inhibit rhythmic swallowing in the rat. Am J Physiol Regul Integr Comp Physiol. 295**,** R1050-9 DOI: 10.1152/ajpregu.90407.2008.

Barraco, R., el-Ridi, M., Ergene, E., Parizon, M., Bradley, D., 1992. An atlas of the rat subpostremal nucleus tractus solitarius. Brain Res Bull. 29**,** 703-65.

Blevins, J.E., Eakin, T.J., Murphy, J.A., Schwartz, M.W., Baskin, D.G., 2003. Oxytocin innervation of caudal brainstem nuclei activated by cholecystokinin. Brain Res. 993**,** 30-41.

Bonnet, M.S., Pecchi, E., Trouslard, J., Jean, A., Dallaporta, M., Troadec, J.D., 2009. Central nesfatin-1-expressing neurons are sensitive to peripheral inflammatory stimulus. J Neuroinflammation. 6**,** 27 DOI: 10.1186/1742-2094-6-27.

Bonnet, M.S., Djelloul, M., Tillement, V., Tardivel, C., Mounien, L., Trouslard, J., Troadec, J.D., Dallaporta, M., 2013. Central NUCB2/Nesfatin-1-expressing neurones belong to the hypothalamic-brainstem circuitry activated by hypoglycaemia. J Neuroendocrinol. 25**,** 1-13 DOI: 10.1111/j.1365-2826.2012.02375.x.

Chung, Y., Jung, E., Kim, H., Kim, J., Yang, H., 2013. Expression of Nesfatin-1/NUCB2 in Fetal, Neonatal and Adult Mice. Dev Reprod. 17**,** 461-7 DOI: 10.12717/dr.2013.17.4.461.

Dogan, U., Bulbuller, N., Cakir, T., Habibi, M., Mayir, B., Koc, U., Aslaner, A., Ellidag, H.Y., Gomceli, I., 2016. Nesfatin-1 hormone levels in morbidly obese patients after laparoscopic sleeve gastrectomy. Eur Rev Med Pharmacol Sci. 20**,** 1023-31.

Feijoo-Bandin, S., Rodriguez-Penas, D., Garcia-Rua, V., Mosquera-Leal, A., Otero, M.F., Pereira, E., Rubio, J., Martinez, I., Seoane, L.M., Gualillo, O., Calaza, M., Garcia-Caballero, T., Portoles, M., Rosello-Lleti, E., Dieguez, C., Rivera, M., Gonzalez-Juanatey, J.R., Lago, F., 2013. Nesfatin-1 in human and murine cardiomyocytes: synthesis, secretion, and mobilization of GLUT-4. Endocrinology. 154**,** 4757-67 DOI: 10.1210/en.2013-1497.

Felix, B., Jean, A., Roman, C., 2006. Leptin inhibits swallowing in rats. Am J Physiol Regul Integr Comp Physiol. 291**,** R657-63 DOI: 10.1152/ajpregu.00560.2005.

Gimpl, G., Fahrenholz, F., 2001. The oxytocin receptor system: structure, function, and regulation. Physiol Rev. 81**,** 629-83.

Goebel-Stengel, M., Wang, L., 2013. Central and peripheral expression and distribution of NUCB2/nesfatin-1. Curr Pharm Des. 19**,** 6935-40.

Goebel, M., Stengel, A., Wang, L., Tache, Y., 2011. Central nesfatin-1 reduces the nocturnal food intake in mice by reducing meal size and increasing inter-meal intervals. Peptides. 32**,** 36-43 DOI: 10.1016/j.peptides.2010.09.027.

Jean, A., 2001. Brain stem control of swallowing: neuronal network and cellular mechanisms. Physiol Rev. 81**,** 929-69.

Kobashi, M., Xuan, S.Y., Fujita, M., Mitoh, Y., Matsuo, R., 2010. Central ghrelin inhibits reflex swallowing elicited by activation of the superior laryngeal nerve in the rat. Regul Pept. 160**,** 19-25 DOI: 10.1016/j.regpep.2009.12.014.

Kobashi, M., Mizutani, S., Fujita, M., Mitoh, Y., Shimatani, Y., Matsuo, R., 2014. Central orexin inhibits reflex swallowing elicited by the superior laryngeal nerve via caudal brainstem in the rat. Physiol Behav. 130**,** 6-12 DOI: 10.1016/j.physbeh.2014.03.009.

Kobashi, M., Mizutani, S., Fujita, M., Mitoh, Y., Shimatani, Y., Matsuo, R., 2017. Central glucagon like peptide-1 inhibits reflex swallowing elicited by the superior laryngeal nerve via caudal brainstem in the rat. Brain Res. 1671**,** 26-32 DOI: 10.1016/j.brainres.2017.07.004.

Kublaoui, B.M., Gemelli, T., Tolson, K.P., Wang, Y., Zinn, A.R., 2008. Oxytocin deficiency mediates hyperphagic obesity of Sim1 haploinsufficient mice. Mol Endocrinol. 22**,** 1723-34 DOI: 10.1210/me.2008-0067.

Landgraf, R., Malkinson, T., Horn, T., Veale, W.L., Lederis, K., Pittman, Q.J., 1990. Release of vasopressin and oxytocin by paraventricular stimulation in rats. Am J Physiol. 258**,** R155-9.

Maejima, Y., Sedbazar, U., Suyama, S., Kohno, D., Onaka, T., Takano, E., Yoshida, N., Koike, M., Uchiyama, Y., Fujiwara, K., Yashiro, T., Horvath, T.L., Dietrich, M.O., Tanaka, S., Dezaki, K., Oh, I.S., Hashimoto, K., Shimizu, H., Nakata, M., Mori, M., Yada, T., 2009. Nesfatin-1-regulated oxytocinergic signaling in the paraventricular nucleus causes anorexia through a leptin-independent melanocortin pathway. Cell Metab. 10**,** 355-65 DOI: 10.1016/j.cmet.2009.09.002.

Mohan, H., Unniappan, S., 2012. Ontogenic pattern of nucleobindin-2/nesfatin-1 expression in the gastroenteropancreatic tissues and serum of Sprague Dawley rats. Regul Pept. 175**,** 61-9 DOI: 10.1016/j.regpep.2012.02.006.

Mostafeezur, R.M., Zakir, H.M., Takatsuji, H., Yamada, Y., Yamamura, K., Kitagawa, J., 2012. Cannabinoids facilitate the swallowing reflex elicited by the superior laryngeal nerve stimulation in rats. PLoS One. 7**,** e50703 DOI: 10.1371/journal.pone.0050703.

Nakata, M., Gantulga, D., Santoso, P., Zhang, B., Masuda, C., Mori, M., Okada, T., Yada, T., 2016. Paraventricular NUCB2/Nesfatin-1 Supports Oxytocin and Vasopressin Neurons to Control Feeding Behavior and Fluid Balance in Male Mice. Endocrinology. 157**,** 2322-32 DOI: 10.1210/en.2015-2082.

Oh-I, S., Shimizu, H., Satoh, T., Okada, S., Adachi, S., Inoue, K., Eguchi, H., Yamamoto, M., Imaki, T., Hashimoto, K., Tsuchiya, T., Monden, T., Horiguchi, K., Yamada, M., Mori, M., 2006. Identification of nesfatin-1 as a satiety molecule in the hypothalamus. Nature. 443**,** 709-12 DOI: 10.1038/nature05162.

Olson, B.R., Drutarosky, M.D., Chow, M.S., Hruby, V.J., Stricker, E.M., Verbalis, J.G., 1991. Oxytocin and an oxytocin agonist administered centrally decrease food intake in rats. Peptides. 12**,** 113-8.

Price, C.J., Hoyda, T.D., Samson, W.K., Ferguson, A.V., 2008. Nesfatin-1 influences the excitability of paraventricular nucleus neurones. J Neuroendocrinol. 20**,** 245-50 DOI: 10.1111/j.1365-2826.2007.01641.x.

Ramanjaneya, M., Chen, J., Brown, J.E., Tripathi, G., Hallschmid, M., Patel, S., Kern, W., Hillhouse, E.W., Lehnert, H., Tan, B.K., Randeva, H.S., 2010. Identification of nesfatin-1 in human and murine adipose tissue: a novel depot-specific adipokine with increased levels in obesity. Endocrinology. 151**,** 3169-80 DOI: 10.1210/en.2009-1358.

Ramesh, N., Gawli, K., Pasupulleti, V.K., Unniappan, S., 2017. Metabolic and Cardiovascular Actions of Nesfatin-1: Implications in Health and Disease. Curr Pharm Des. 23**,** 1453-1464 DOI: 10.2174/1381612823666170130154407.

Rinaman, L., 1998. Oxytocinergic inputs to the nucleus of the solitary tract and dorsal motor nucleus of the vagus in neonatal rats. J Comp Neurol. 399**,** 101-9.

Rosen, G.J., de Vries, G.J., Goldman, S.L., Goldman, B.D., Forger, N.G., 2008. Distribution of oxytocin in the brain of a eusocial rodent. Neuroscience. 155**,** 809-17 DOI: 10.1016/j.neuroscience.2008.05.039.

Saito, R., Sonoda, S., Ueno, H., Motojima, Y., Yoshimura, M., Maruyama, T., Hashimoto, H., Tanaka, K., Yamamoto, Y., Kusuhara, K., Ueta, Y., 2017. Involvement of central nesfatin-1 neurons on oxytocin-induced feeding suppression in rats. Neurosci Lett. 655**,** 54-60 DOI: 10.1016/j.neulet.2017.06.049.

Shimizu, H., Oh, I.S., Hashimoto, K., Nakata, M., Yamamoto, S., Yoshida, N., Eguchi, H., Kato, I., Inoue, K., Satoh, T., Okada, S., Yamada, M., Yada, T., Mori, M., 2009a. Peripheral administration of nesfatin-1 reduces food intake in mice: the leptin-independent mechanism. Endocrinology. 150**,** 662-71 DOI: 10.1210/en.2008-0598.

Shimizu, H., Oh, I.S., Okada, S., Mori, M., 2009b. Nesfatin-1: an overview and future clinical application. Endocr J. 56**,** 537-43.

St-Pierre, D.H., Martin, J., Shimizu, H., Tagaya, Y., Tsuchiya, T., Marceau, S., Biertho, L., Bastien, M., Caron-Cantin, S.M., Simard, S., Richard, D., Cianflone, K., Poirier, P., 2016. Association between nesfatin-1 levels and metabolic improvements in severely obese patients who

underwent biliopancreatic derivation with duodenal switch. Peptides. 86**,** 6-12 DOI: 10.1016/j.peptides.2016.09.014.

Stengel, A., Goebel, M., Wang, L., Rivier, J., Kobelt, P., Monnikes, H., Lambrecht, N.W., Tache, Y., 2009. Central nesfatin-1 reduces dark-phase food intake and gastric emptying in rats: differential role of corticotropin-releasing factor2 receptor. Endocrinology. 150**,** 4911-9 DOI: 10.1210/en.2009-0578.

Takayanagi, Y., Kasahara, Y., Onaka, T., Takahashi, N., Kawada, T., Nishimori, K., 2008. Oxytocin receptor-deficient mice developed late-onset obesity. Neuroreport. 19**,** 951-5 DOI: 10.1097/WNR.0b013e3283021ca9.

Tsuchiya, T., Shimizu, H., Yamada, M., Osaki, A., Oh, I.S., Ariyama, Y., Takahashi, H., Okada, S., Hashimoto, K., Satoh, T., Kojima, M., Mori, M., 2010. Fasting concentrations of nesfatin-1 are negatively correlated with body mass index in non-obese males. Clin Endocrinol (Oxf). 73**,** 484-90 DOI: 10.1111/j.1365-2265.2010.03835.x.

Uchoa, E.T., Zahm, D.S., de Carvalho Borges, B., Rorato, R., Antunes-Rodrigues, J., Elias, L.L., 2013. Oxytocin projections to the nucleus of the solitary tract contribute to the increased meal-related satiety responses in primary adrenal insufficiency. Exp Physiol. 98**,** 1495-504 DOI: 10.1113/expphysiol.2013.073726.

Wang, Y., Li, Z., Zhang, X., Xiang, X., Li, Y., Mulholland, M.W., Zhang, W., 2016. Nesfatin-1 promotes brown adipocyte phenotype. Sci Rep. 6**,** 34747 DOI: 10.1038/srep34747.

Yosten, G.L., Samson, W.K., 2010. The anorexigenic and hypertensive effects of nesfatin-1 are reversed by pretreatment with an oxytocin receptor antagonist. Am J Physiol Regul Integr Comp Physiol. 298**,** R1642-7 DOI: 10.1152/ajpregu.00804.2009.

Zhang, A.Q., Li, X.L., Jiang, C.Y., Lin, L., Shi, R.H., Chen, J.D., Oomura, Y., 2010. Expression of nesfatin-1/NUCB2 in rodent digestive system. World J Gastroenterol. 16**,** 1735-41.

Figure 1

Click here to download high resolution image

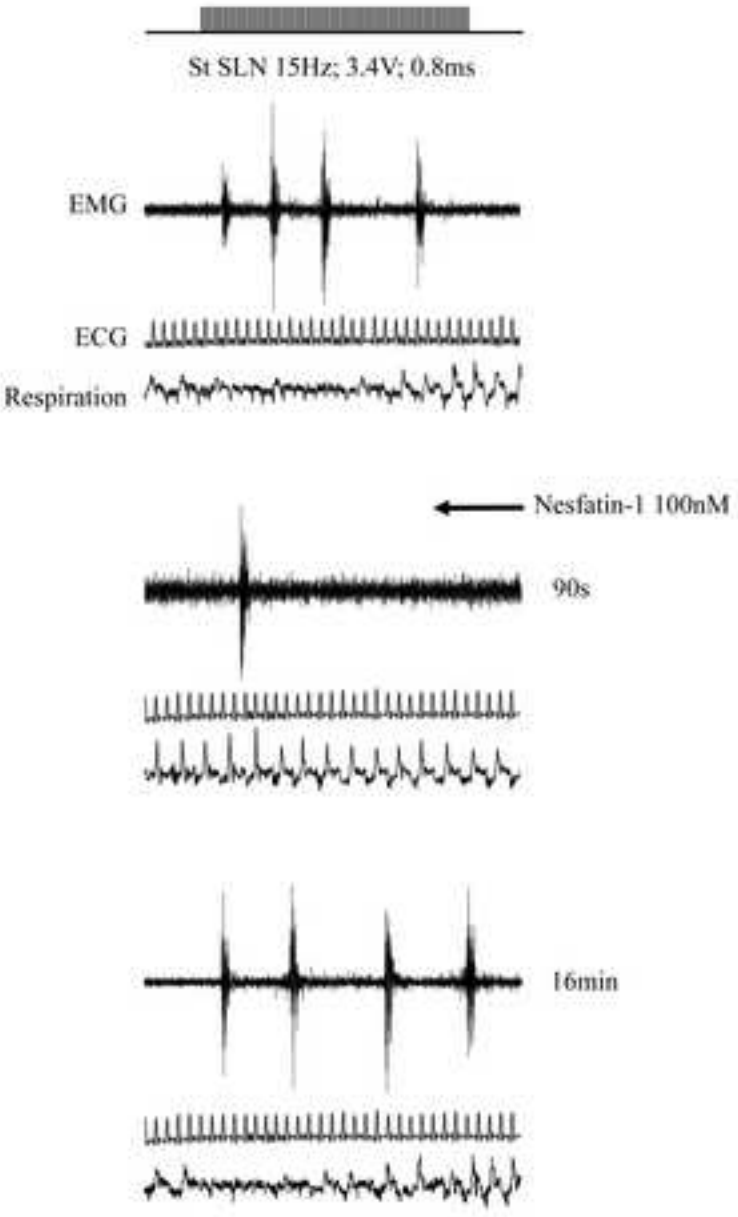

Figure 2

Click here to download high resolution image

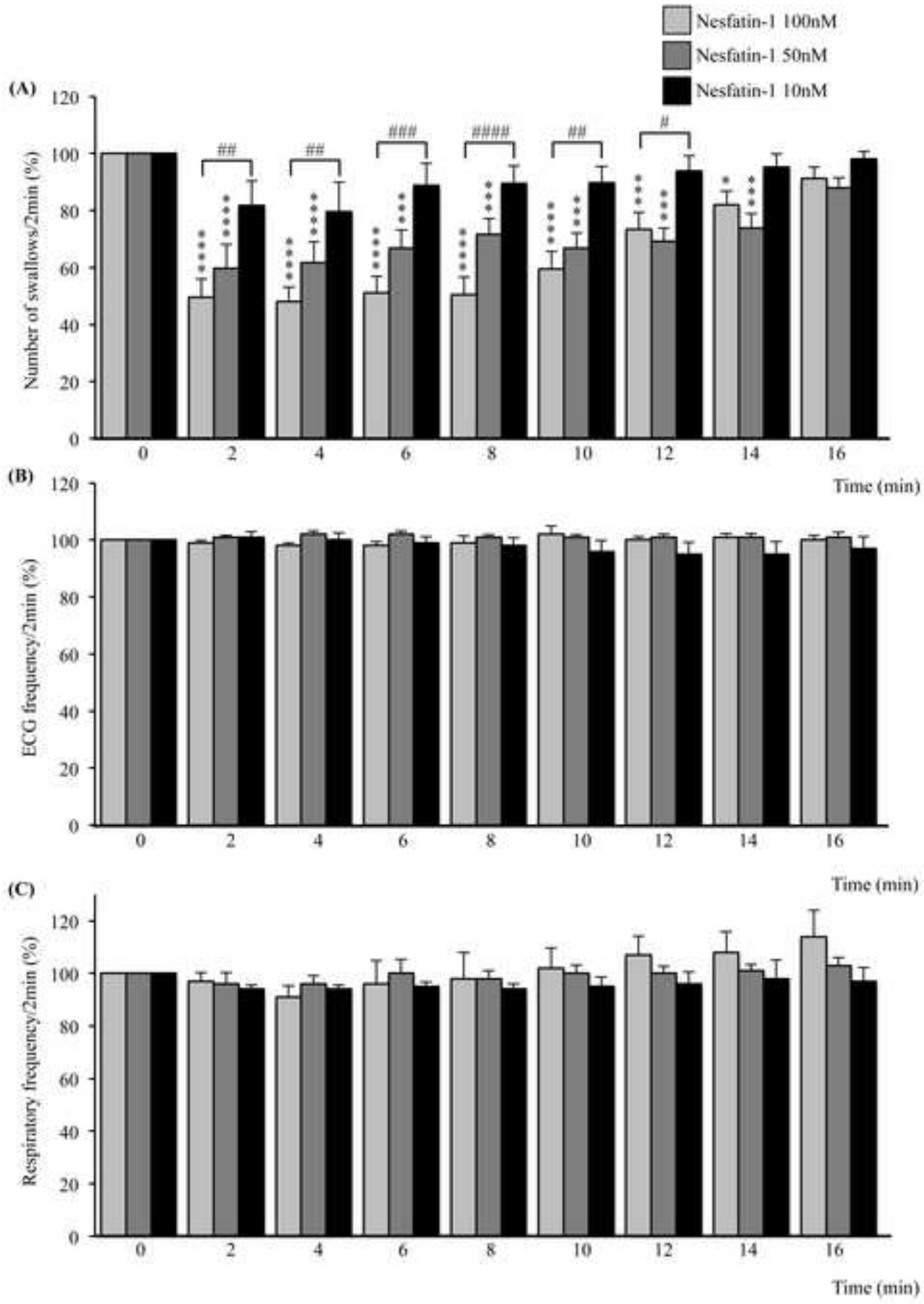

Figure 3

Click here to download high resolution image

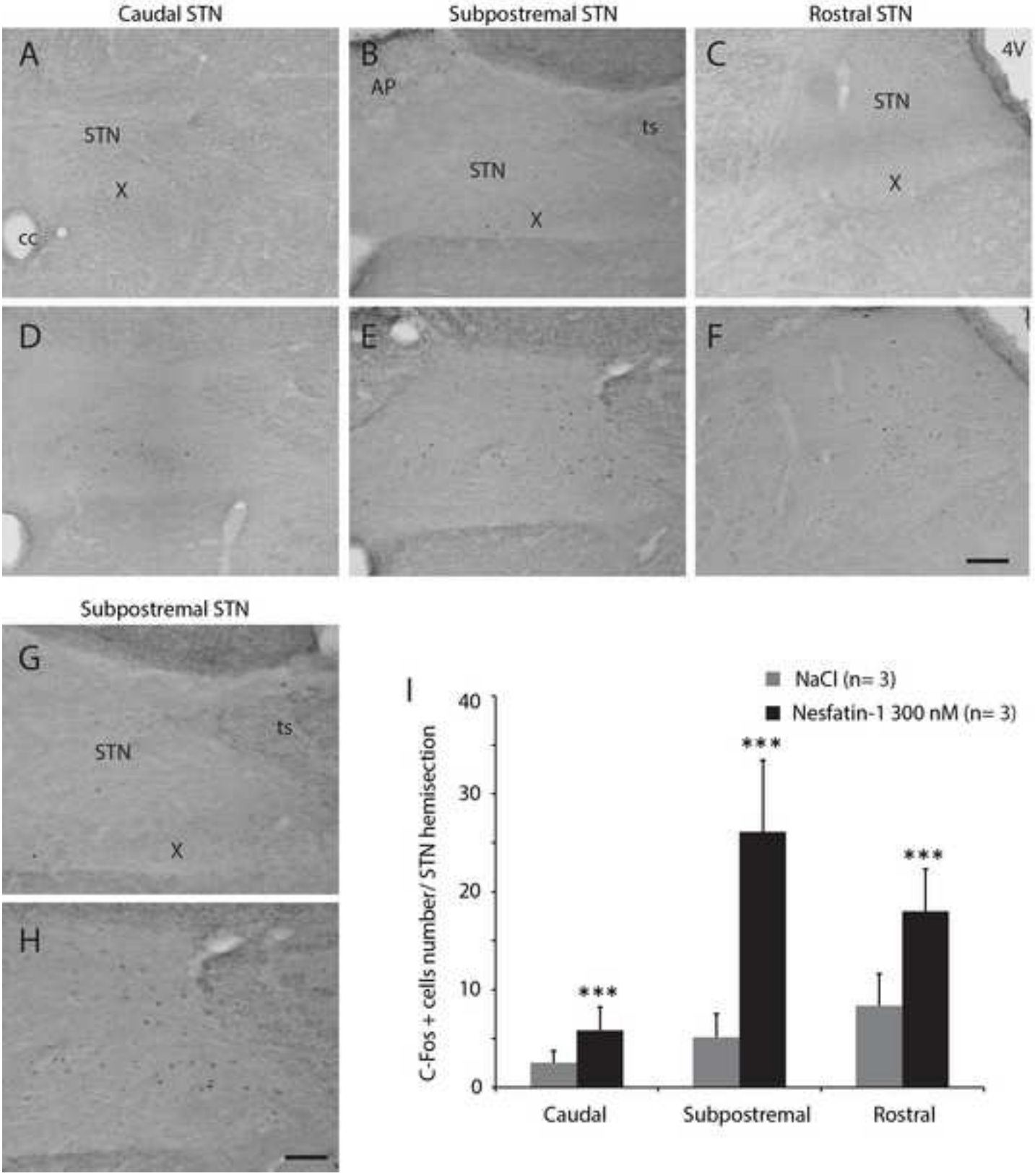

Figure 4

Click here to download high resolution image

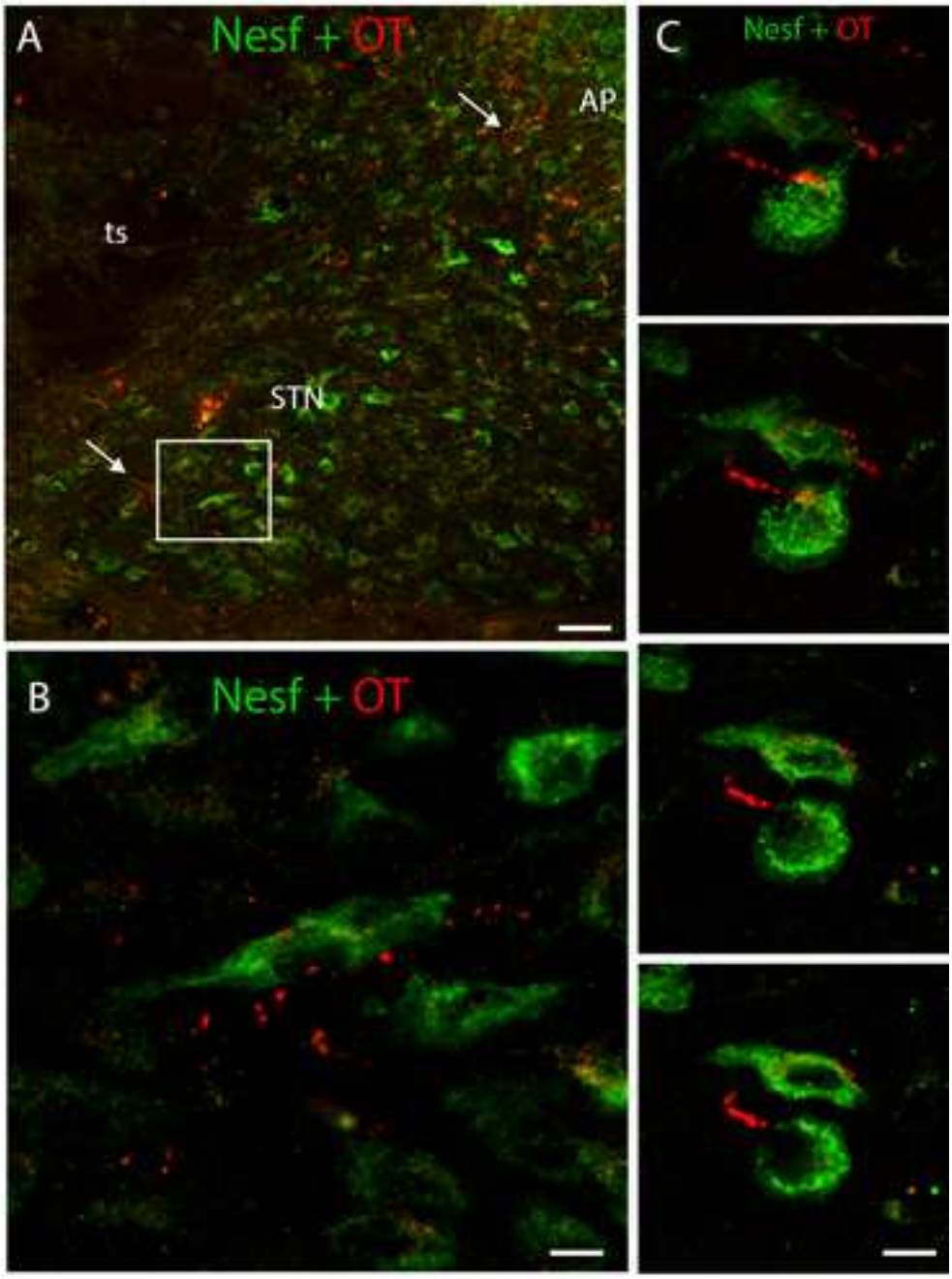

Figure 5

Click here to download high resolution image

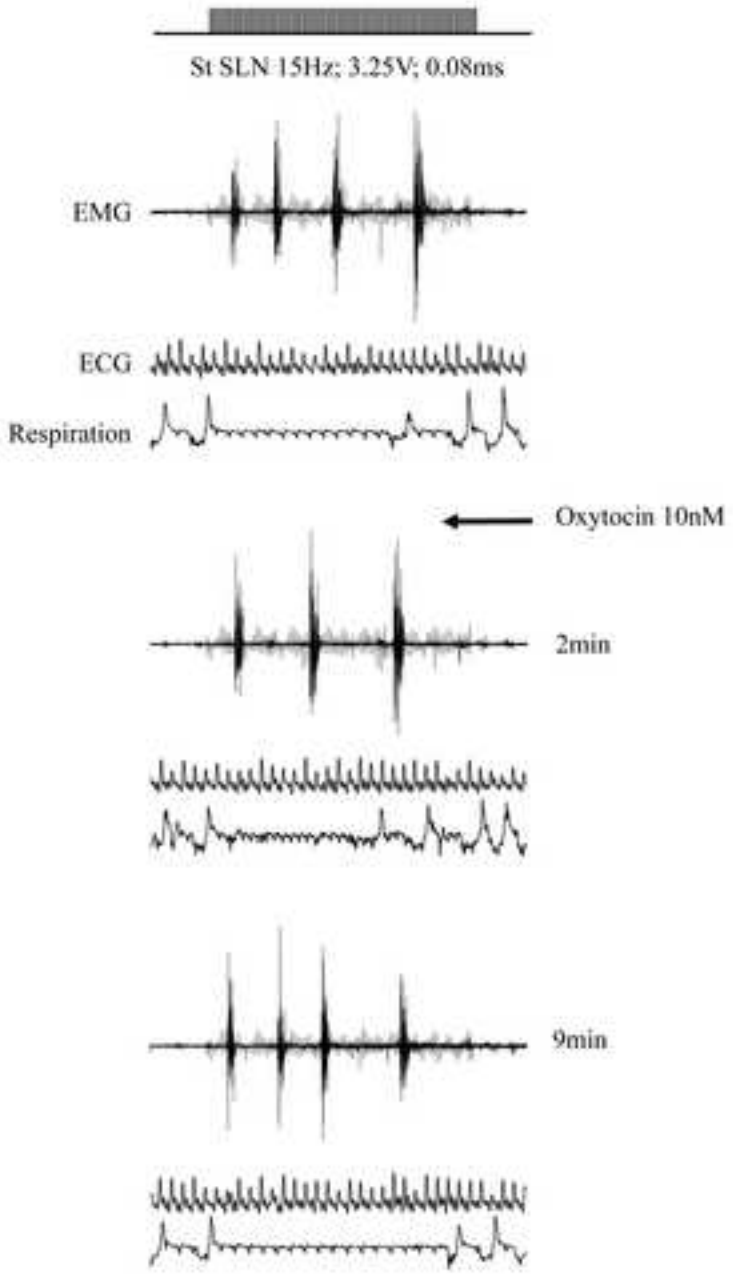

Figure 6

Click here to download high resolution image

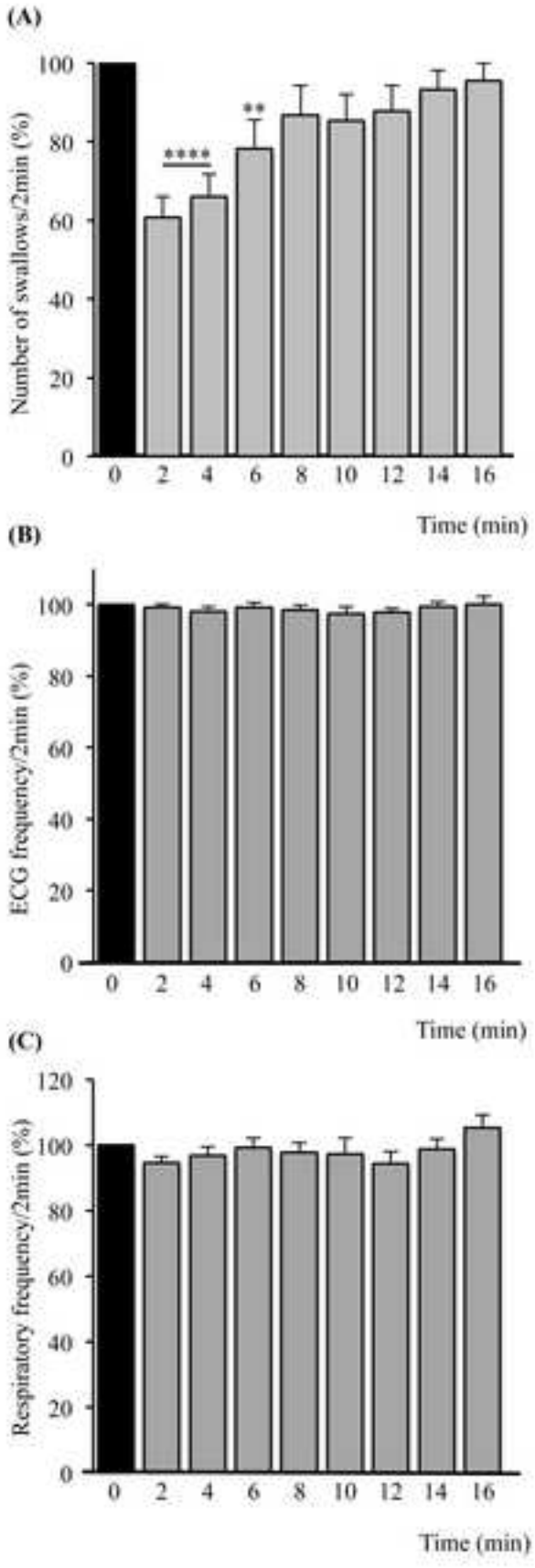

Figure 7

Click here to download high resolution image